N. Jb. Geol. Paläont. Abh. 293/1 (2019), 37–56
Stuttgart, July 2019

Article

Early Changhsingian (Late Permian) ammonoids from NW Iran

Dieter Korn, Abbas Ghaderi, and Nahideh Ghanizadeh Tabrizi

With 25 figures

Abstract: Early Changhsingian ammonoids from the Transcaucasus-NW Iranian region are poorly known. Here we revise the ammonoids of this interval based on new findings in sections of the Aras Valley and Ali Bashi Mountains of the Julfa region, NW Iran. We revise the ceratitid genera *Phisonites*, *Iranites*, *Shevyrevites* and *Dzhulfites*. We introduce the new genus *Araxoceltites* with the three new species *A. sanestapanus*, *A. laterocostatus* and *A. cristatus*.

Key words: Late Permian, Ammonoidea, Iran, stratigraphy, diversity.

1. Introduction

Late Permian (Lopingian) ammonoids are remarkable for their high overturn rates, which stand in contrast to the Early and Middle Permian, during which the group evolved considerably slowly on the substage and stage levels (e.g., Miller & Furnish 1940; Ruzhencev 1952; Ruzhencev 1956; Leonova 2002). The Late Permian is, after the end-Guadalupian extinction event that caused a significant extinction of the goniatitid ammonoids, characterized by the presence of ammonoid assemblages dominated by the order Ceratitida (e.g., Ruzhencev 1962; Ruzhencev 1963; Zhao et al. 1978). Wuchiapingian ammonoid assemblages are dominated by members of the superfamily Otoceratoidea, while the Changhsingian assemblages are almost entirely composed of the superfamily Xenodiscoidea (e.g., Ruzhencev & Shevyrev 1965; Zhao et al. 1978; Leonova 2002). During the Changhsingian, the otoceratids existed only as a ghost lineage (e.g., Kummel 1972). The abrupt change in the composition of ammonoid assemblages between the two stages has not been explained so far.

Early Changhsingian ammonoids are known in greater diversity from only two regions worldwide, the Transcaucasian-NW Iranian region and South China. However, while the South Chinese assemblages show a high species richness, those from the Transcaucasus are comparatively poor. In their monograph describing the sections in Armenia and Azerbaijan, for instance, Ruzhencev & Shevyrev (1965) listed only eight xenodiscid species from this interval. This is in striking contrast to the late Changhsingian, from where alone nearly 30 species are known from the *Paratirolites* Limestone of NW Iran (Korn et al. 2016). A diversity analysis showed that the ammonoid diversity is increasing towards the top of the formation (Kiessling et al. 2018).

During our field study of the Permian-Triassic boundary beds of NW Iran (Fig. 1), we measured and sampled several sections (Aras Valley, several parallel sections in the Ali Bashi Mountains, Zal) in great detail (applying bed-by-bed sampling) with the focus on petrography and microfacies characteristics (Leda et al. 2014), conodont stratigraphy (Ghaderi 2014; Ghaderi et al. 2014b; Isaa et al. 2016), stable isotopes (Schobben et al. 2014; Schobben et al. 2015; Schobben et al. 2016; Schobben et al. 2019), brachiopods (Ghaderi et al. 2014a) and ammonoids (Ghaderi et al. 2014b; Korn et al. 2016). Within this multidisciplinary project, we also collected a number of ammonoids from the early Changhsingian Zal Member of the Ali Bashi Formation, which are described below.

DOI: 10.1127/njgpa/2019/0829

www.schweizerbart.de
0077-7749/2019/0829 $ 5.00

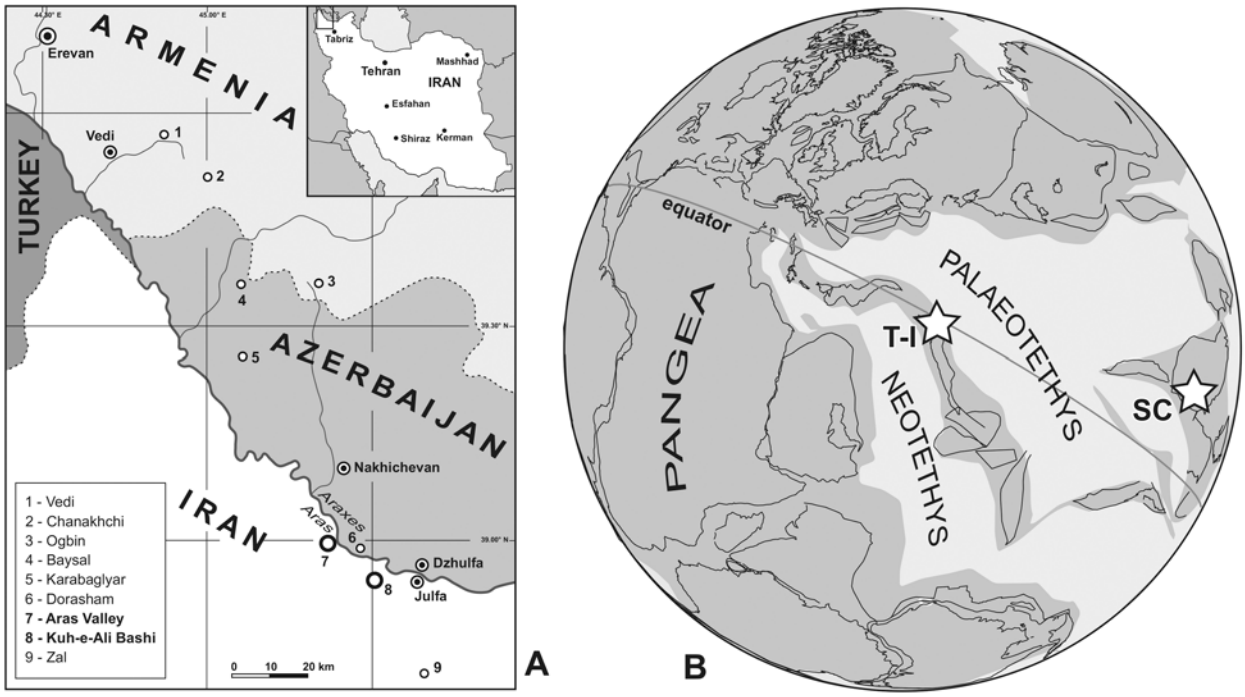

Fig. 1. Geographic position of Permian-Triassic boundary sections in the Transcaucasus-NW Iran region (after Arakelyan et al. 1965) and palaeogeographic position of the Julfa region (after Stampfli & Borel 2002).

2. Material

The studied material comes from the early Changhsingian Zal Member (i.e. the lower part of the Ali Bashi Formation), which has a position between two units of nodular or platy limestone: the upper part of Julfa Formation below and *Paratirolites* Limestone above (Ghaderi et al. 2014b). The Zal Member is mainly composed of light to dark grey, reddish or purple shales with the intercalation of marly limestone beds or packages of thin bedded limestone beds (Fig. 2). Several of the beds yielded macrofossils, but ammonoids could be collected only occasionally from a few levels. The member is, geographically, restricted to a rather small area between the northern side of the Araxes (= Aras) river and the village of Zal about 30 kilometres to the South (Fig. 1). At most places, the member is covered by scree; only occasionally the entire member is exposed.

Our material, consisting of 126 specimens, comes from the following localities (for a detailed outline of the stratigraphic succession, see Ghaderi et al. 2014b; Leda et al. 2014):

Aras Valley section (39.0154° N, 45.4345° E): This section was described for the first time by Ghaderi et al. (2014b) and Leda et al. (2014); it is situated about 19 km WNW of the towns of Dzhulfa and Julfa in a dry small side valley west of the Aras (Araxes) River. The outcrop has a position approximately 2 km north-west of the Dorasham I section of Ruzhencev et al. (1965) and Kotlyar et al. (1983). A nearly complete Wuchiapingian and Changhsingian succession is exposed at this locality with a good outcrop of the Zal Member over an extension of 200 m. The member has a thickness of 9.35 m; we collected 77 specimens.

Ali Bashi 1 section (38.9397° N, 45.5197° E): It corresponds to Locality 1 described in some detail by Teichert et al. (1973). The entire Changhsingian succession is exposed in this section and allows a detailed study. The Zal Member has a thickness of about 12 m; we collected five specimens.

Ali Bashi 4 section (38.9416° N, 45.5158° E): Locality 4 of Teichert et al. (1973) is the section described in detail by Stepanov et al. (1969) and Ghaderi et al. (2014b). It is the most complete of all the sections in the Ali Bashi Mountains. The Zal Member has a thickness of 12.40 m; we collected 14 specimens.

Ali Bashi N section (38.9456° N, 45.5137° E): This section has only rarely been studied previously (Ghaderi et al. 2014b; Korn et al. 2016). It begins in the higher portion of the Zal Member and ranges into the Triassic Elikah Formation; we collected one specimen.

Zal section (38.7327° N, 45.5795° E): The type locality of the Zal Member shows a succession that resembles, in spite of about twenty kilometres distance, the Ali Bashi and Aras Valley sections. The Zal Member has a thickness of 12.40 m; we collected 29 specimens.

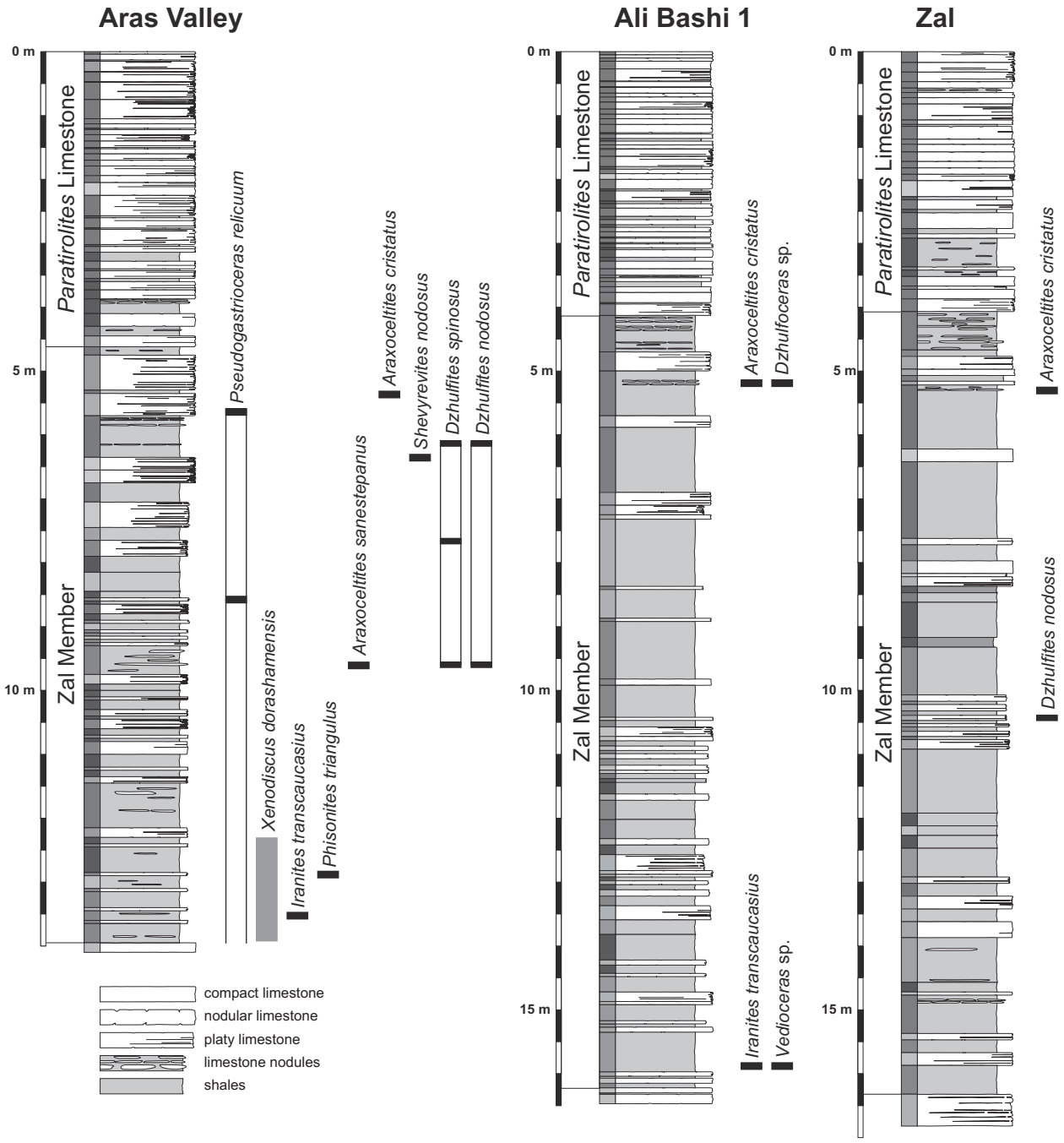

Fig. 2. Columnar sections of the Zal Member with the in-situ collected ammonoid specimens.

In total, 126 ammonoid specimens of the Zal Member were collected, of which only a few were collected in-situ (Fig. 2). The specimens belong to the following species:

Pseudogastrioceras relicuum Korn & Ghaderi (in Korn et al. 2016)	– 8 specimens
Xenodiscus dorashamensis Shevyrev, 1965	– 16 specimens
Xenodiscus sp.	– 1 specimen
Phisonites triangulus Shevyrev, 1965	– 4 specimens
Iranites transcaucasius (Shevyrev, 1965)	– 9 specimens
Shevyrevites shevyrevi Teichert & Kummel (in Teichert et al. 1973)	– 3 specimens
Shevyrevites nodosus Shevyrev, 1965	– 1 specimen
Araxoceltites cristatus n. gen. n. sp.	– 37 specimens
Araxoceltites sanestapanus n. gen. n. sp.	– 13 specimens
Araxoceltites laterocostatus n. gen. n. sp.	– 2 specimens
Dzhulfites spinosus Shevyrev, 1965	– 7 specimens
Dzhulfites nodosus Shevyrev, 1965	– 23 specimens
Vedioceras sp.	– 1 specimen
Dzhulfoceras sp.	– 1 specimen

Unfortunately, most of the specimens are incomplete of just whorl fragments. Even when the conch is rather complete, the specimens suffered from distortion. Many of them are weathered because they are float collections.

3. Ammonoid zonation within the Zal Member

In accordance to previous articles (Ghaderi et al. 2014b; Leda et al. 2014; Korn et al. 2016), we orientate the position of the respective fossil horizons at the end-Permian extinction horizon, which is the top of the *Paratirolites* Limestone. All fossil horizons mentioned here are thus given in metres with a minus prefix.

The Wuchiapingian–Changhsingian transition is poorly known in the Transcaucas and NW Iran. The highest occurrence of the araxoceratid *Vescotoceras* is recorded, in the Aras Valley section, at the top of the Julfa Formation. In the sections at Dorasham on the north bank of the Araxes (= Aras) river in Azerbaijan, Ruzhencev & Shevyrev (1965) subdivided the interval between the beds with *Vedioceras* (= late Wuchiapingian) and *Paratirolites* (= late Changhsingian) into four ammonoid zones, characterised by the genera *Phisonites*, "*Tompophiceras*", *Dzhulfites* and "*Bernhardites*". After a revision of these genera by Teichert & Kummel (in Teichert et al. 1973), four biozones characterised by *Phisonites triangulus*, *Iranites transcaucasius*, *Dzhulfites nodosus* and *Shevyrevites shevyrevi* were established (Kotlyar et al. 1983).

The study of the NW Iranian sections showed that the subdivision developed in the Dorasham section can largely be confirmed, but modifications have to be done (Fig. 2).

1. *Iranites transcaucasius–Phisonites triangulus* Zone. – The lowermost part of the Ali Bashi Formation contains ammonoid assemblages in low diversity and rather poor preservation. *Iranites transcaucasius* and *Phisonites triangulus* occur, together with other smooth ceratitic ammonoids, at the base of the Zal Member in the Aras Valley section. According to our collections, the two zones proposed by Ruzhencev & Shevyrev (1965) cannot be separated. *Phisonites triangulus* occurs, in the Aras Valley section, in a single thin limestone bed 12.90 m below the extinction horizon. *Iranites transcaucasius* was collected by us already below this bed at −13.50 m, and hence the two zones are merged here.

A fragment of *Vedioceras* sp. in shales at the base of the Ali Bashi Formation in the Ali Bashi 1 section demonstrates that the change from *Vedioceras*-dominated faunas of the Wuchiapingian to the xenodiscid-dominated assemblages of the Changhsingian is probably not abrupt. It can, however, not be excluded that the specimen was reworked, as it is rather strongly corroded.

2. *Dzhulfites nodosus* Zone. – The zone is best recorded in the Aras Valley and Zal sections. In the Aras Valley section, *Dzhulfites nodosus*, *D. spinosus* and *Araxoceltites sanestapanus* occur at −9.50 m. In the Zal section, the horizon with the two *Dzhulfites* species has a position at −10.30 m. A second horizon in the Aras Valley section lies at −8.20 m, where *Pseudogastrioceras relicuum* occurs with specimens of *Dzhulfites* and *Araxoceltites*. Higher horizons with *Dzhulfites* in the Aras Valley section occur at −7.60 and −6.15 m. The zone is thus rather well-represented in the sections, although diversity is rather low with a total of five species.

3. *Shevyrevites shevyrevi* Zone. – In the Aras Valley, Ali Bashi and Zal sections, there is a rather fossiliferous purple shale package about 0.80 m below the base of the *Paratirolites* Limestone. Unfortunately, the ammonoid specimens are mostly fragmented in this bed and only rarely allow the study of more than one volution. *Araxoceltites cristatus* is by far the most common species; it is accompanied by specimens of *Shevyrevites* and rare *Dzhulfites* species. *Shevyrevites* has obviously only a very limited stratigraphic range and oc-

curs only in this thin interval at the top of the Zal Member below the *Paratirolites* Limestone. In the Ali Bashi 1 section, a specimen of *Dzhulfoceras* sp. was recorded in this horizon at −5.20. The preservation of this small specimen resembles the other ammonoids from this horizon; reworking from much lower beds is not likely.

4. Systematic descriptions

Description of the ammonoids largely follows the scheme and terminology, which was proposed by Korn (2010) for Palaeozoic ammonoids. For the shape of the cross sections, an additional explanation of terminology was given by Korn & Ghaderi (in Korn et al. 2016) Korn et al. (2016). This distinguishes between trapezoidal, quadrate, subtrapezoidal, circular and oval (Fig. 3). The terminology of the suture line follows Korn et al. (2003), meaning that a difference between an A-mode (goniatitic) and U-mode (prolecanitic and thus also ceratitic) sutural ontogeny, as proposed by Schindewolf (1929), is not accepted. The sutural elements described here are therefore external (E), adventive (A), lateral (L), umbilical (U) and internal (I) lobes.

Abbreviations for the affiliation of the material are for the following institutions: MB.C. – Cephalopod collection of the Museum für Naturkunde, Berlin; PIN – Palaeontological Institute of the Academy of Sciences, Moscow; MCZ – Museum of Comparative Zoology, Harvard University.

Order Goniatitida Hyatt, 1884
Suborder Goniatitina Hyatt, 1884
Superfamily Neoicoceratoidea Hyatt, 1900
Family Paragastrioceratidae Ruzhencev, 1951
Subfamily Pseudogastrioceratinae Furnish, 1966
For the composition of the subfamily,
see Korn & Ghaderi (in Korn et al. 2016).

Genus *Pseudogastrioceras* Spath, 1930

For the composition of the genus, see Korn & Ghaderi (in Korn et al. 2016).

Pseudogastrioceras relicuum Korn & Ghaderi
(in Korn et al. 2016)
Figs. 4, 5

2016 *Pseudogastrioceras relicuum* Korn & Ghaderi (in Korn et al.), p. 852, text-fig. 12.

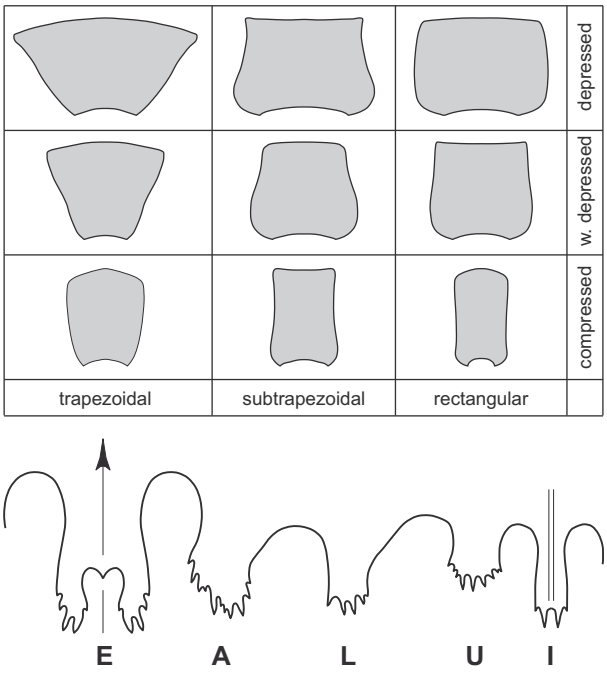

Fig. 3. Descriptive terms for the whorl profiles and suture line terminology of the ammonoids described here.

Holotype: Specimen MB.C.25173; illustrated by Korn & Ghaderi (in Korn et al. 2016, text-fig. 12).

Type locality and horizon: Ali Bashi N section; float from *Paratirolites* Limestone.

Material: Eight mostly fragmentary specimens (Aras Valley: 6; Ali Bashi 1: 1; Zal: 1).

Diagnosis (emended from Korn & Ghaderi in Korn et al. 2016): *Pseudogastrioceras* with moderately large conch; diameter attaining 150 mm. Conch shape thinly discoidal (ww/dm~= 0.40–0.45), involute (uw/dm ~ 0.05) with converging flanks and broadly rounded venter. Ornament with about 15–20 faint spiral lines on the venter; spiral lines coarse and sharp in the adult stage.

Description: MB.C.29135 is an incomplete steinkern specimen but allows the study of some conch and ornament characters (Fig. 4). It is largely septate and the maximum phragmocone diameter is 90 mm. Septal crowding indicates adulthood of the specimen, which might have reached a conch diameter of 150 mm. The specimen has the typical shape and ornament of a *Pseudogastrioceras*. There are rather coarse spiral lines on the outer flank and venter; their total number is about 20.

The suture line of the large specimen (47 mm whorl height) shows an outline typical for the genus (Fig. 5). The rather wide V shaped external lobe has weakly incurved flanks and the median saddle has about half the height of

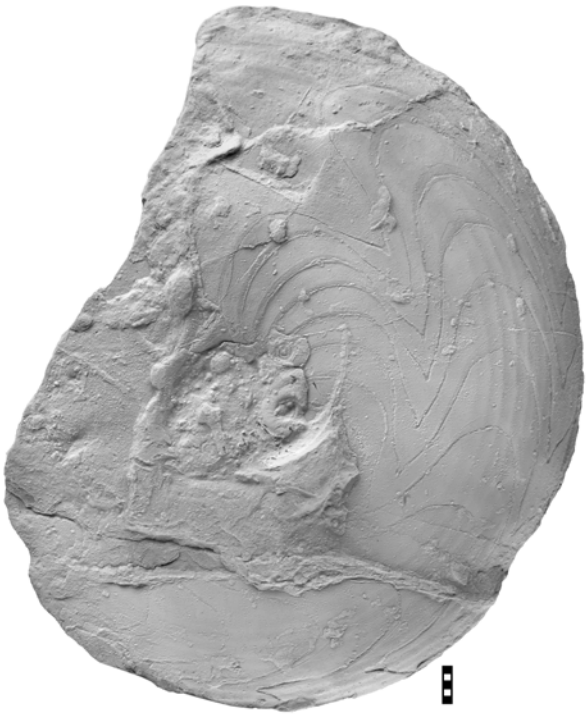

Fig. 4. *Pseudogastrioceras relicuum* Korn & Ghaderi, 2016. Specimen MB.C.29135 from float of the Zal Member in the Aras Valley section. Scale bar units = 1 mm.

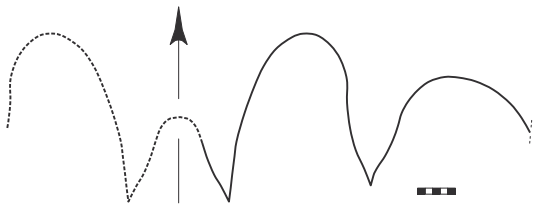

Fig. 5. *Pseudogastrioceras relicuum* Korn & Ghaderi, 2016. Suture line (reversed) of specimen MB.C.29135 from the Aras Valley section, at 47 mm wh. Scale bar units = 1 mm.

the external lobe depth. The V-shaped and nearly symmetric adventive lobe is much smaller than the external lobe. Both lobes are separated by a broadly rounded, dorsally inclined ventrolateral saddle.

Order Ceratitida Hyatt, 1884
Suborder Paraceltitina Shevyrev, 1968
Superfamily Xenodiscoidea Frech, 1902
Family Xenodiscidae Frech, 1902

Diagnosis: Representatives of the superfamily Xenodiscoidea with small to moderately large conch, in which the ontogeny displays up to three stages, beginning with a unsculptured initial stage followed by a juvenile stage with transverse ribs, and an adult stage with weakening of the sculpture. Suture line with unserrated or weakly serrated, short but rather wide external lobe; adventive, lateral and umbilical lobe often multidentate; some species with a simplified suture line without serrations.

Genus *Xenodiscus* Waagen, 1879

Type species: *Xenodiscus plicatus* Waagen, 1879, p. 34; subsequently designated by Waagen (1895, p. 161) = *Ceratites carbonarius* Waagen, 1872, p. 355 (subjective according to Spinosa et al. 1975, p. 270).

Included species:

araxensis: *Xenaspis araxensis* Shevyrev, 1965; Transcaucasia [synonym of *Xenodiscus dorashamensis* Shevyrev, 1965].

besairiei: *Xenodiscus besairiei* Spinosa, Furnish & Glenister, 1975; Madagascar.

carbonarius: *Ceratites carbonarius* Waagen, 1872; Salt Range.

chaotianensis: *Xenodiscus chaotianensis* Zhao, Liang & Zheng, 1978; South China.

dieneri: *Xenodiscus dieneri* Spinosa, Furnish & Glenister, 1975; Tibet.

dorashamensis: *Xenodiscus dorashamensis* Shevyrev, 1965; Transcaucasia.

jubilaearis: *Xenodiscus jubilaearis* Zakharov in Zakharov & Rybalka, 1987; Transcaucasia.

muratai: *Xenodiscus muratai* Bando, 1979; Central Iran.

plicatus: *Xenodiscus plicatus* Waagen, 1879; Salt Range [synonym of *Xenodiscus carbonarius* (Waagen, 1872)].

rotundus: *Xenodiscus rotundus* Haniel, 1915; Timor.

sinensis: *Paraceltitoides sinensis* Zheng & Chen, 1979; NW China.

subcarbonarius: *Xenodiscus subcarbonarius* Zakharov & Pavlov, 1986; Primorie.

wanneri: *Xenodiscus wanneri* Spinosa, Furnish & Glenister, 1975; Coahuila.

xizangensis: *Xenaspis xizangensis* Sheng, 1988; Tibet.

Genus diagnosis: Genus of the Xenodiscidae with moderately large conchs (diameter greater than 50 mm). Conch extremely discoidal (ww/dm commonly 0.15–0.30), evolute (uw/dm generally 0.40–0.60 at maturity), flanks roughly parallel, venter broadly rounded or bluntly angular. Ornament consists often of plications, with variable relief, ranging from coarse and widely spaced to faint and closely spaced.

Xenodiscus dorashamensis Shevyrev, 1965
Figs. 6, 7

1965 *Xenaspis araxensis* Shevyrev, p. 166, pl. 21, fig. 1,
1965 *Xenodiscus dorashamensis* Shevyrev, p. 166, pl. 21 figs. 2, 3.
1973 *Xenodiscus dorashamensis*. – Teichert & Kummel (in Teichert et al.), p. 406, pl. 3, figs. 9–17, text-fig. 11G.
1975 *Xenodiscus dorashamensis*. – Spinosa et al., p. 278.
1979 *Xenodiscus dorashamensis*. – Bando, p. 131, pl. 5, figs. 3, 12.

Holotype: Specimen PIN 1478/68; figured by Shevyrev (1965, pl. 21, fig. 3).

Type locality and horizon: Dorasham 2 (Azerbaijan); *Phisonites triangulus–Iranites transcaucasius* Zone (Late Permian).

Material: Sixteen fragmentary specimens (Aras Valley: 14; Ali Bashi 4: 2).

Diagnosis: *Xenodiscus* with a conch reaching 50 mm dm. All stages with oval, compressed whorl cross section (ww/wh ~ 0.75), rounded venter and moderately wide umbilicus (uw/dm ~ 0.40). Sometimes with faint plications on the inner flank, venter smooth. Prongs of the external lobe usually simple or bifid; altogether 10–15 notches of the E, A and L lobes.

Description: Specimen MB.C.29143.1 is a fragment of a body chamber that reaches a diameter of about 48 mm (Fig. 6 A). It has an oval compressed whorl profile with rounded venter (ww/wh ~ 0.75). Its inner flanks possess broad and rounded plications, which extend with a dorsolateral projection and then wedge out in the midflank area, where they are bent backwards.

A similar conch shape and ornament can be seen in the partly crushed specimen MB.C.29143.2 (31.5 mm conch diameter; Fig. 6C). At 21 mm dm, the ww/dm ratio is 0.74. Its suture line has, at 8 mm whorl height, a parallel-sided external lobe with broad prongs that have four small notches. Generally, the lobes and saddles have vertical flanks; the large adventive lobe and the much smaller lateral lobe are U-shaped with a number of small notches at the base (Fig. 7B).

The suture line of the small specimen MB.C.29142.1 (5.6 mm whorl height) has a nearly parallel-sided external lobe with unsubdivided prongs (Fig. 7C). This lobe has about two thirds of the depth of the large adventive lobe. Both the adventive and the lateral lobes possess a weakly serrated base, but the lateral lobe is much smaller than the adventive lobe. The lobes are separated by weakly inflated, rather narrow saddles.

Fig. 6. *Xenodiscus dorashamensis* Shevyrev, 1965. **A** – Specimen MB.C.29143.1 from float of the Zal Member in the Aras Valley section. **B** – Specimen MB.C.29142.1 from float of the Zal Member in the Aras Valley section. **C** – Specimen MB.C.29143.2 from float of the Zal Member in the Aras Valley section. Scale bar units = 1 mm.

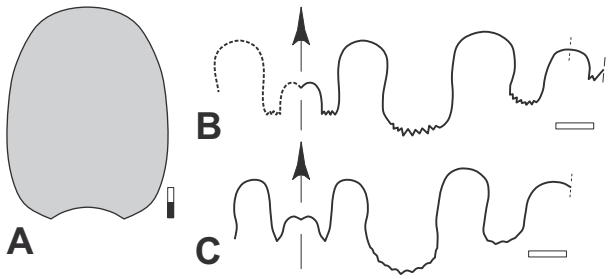

Fig. 7. *Xenodiscus dorashamensis* Shevyrev, 1965 from the Aras Valley section. **A** – Whorl profile of specimen MB.C.29143.1. **B** – Suture line (reversed) of specimen MB.C.29143.2, at 21.0 mm dm, 5.5 mm ww, 7.4 mm wh. **C** – Suture line of specimen MB.C.29142.1, at 4.8 mm ww, 5.6 mm wh. Scale bar units = 1 mm.

Discussion: The relationships between the two species *Xenaspis araxensis* and *Xenodiscus dorashamensis* were discussed in length by Teichert & Kummel (in Teichert et al. 1973) and Spinosa et al. (1975); these authors concluded that the presence of faint plications in the first species do not justify separation. Therefore they proposed *Xenodiscus dorashamensis* to be the valid species and regarded *Xenaspis araxensis* as its synonym. The Transcaucasian species differs from the other species in the genus in the narrower umbilicus (uw/dm ~ 0.40 in *X. dorashamensis* but around 0.50 or more in the other species).

Genus *Phisonites* Shevyrev, 1965

Type species: *Phisonites triangulus* Shevyrev, 1965, by original designation.

Genus diagnosis: Genus of the Xenodiscidae with moderately large conch (diameter reaching 80 mm). Conch discoidal, subevolute; whorl profile almost triangular, venter narrowly rounded, umbilical margin strongly attenuated, umbilical wall high and steep. Shell surface smooth, occasionally with small umbilical tubercles.

Included species:

triangulus: *Phisonites triangulus* Shevyrev, 1965; Transcaucasus.

Phisonites triangulus Shevyrev, 1965
Fig. 8

1965 *Phisonites triangulus* Shevyrev, p. 168, pl. 21, figs. 4, 5.
1973 *Phisonites triangulus*. – Teichert & Kummel (in Teichert et al.), p. 406, pl. 8, figs. 1–8, text-fig. 11L.
2014 *Phisonites triangulus*. – Korn (in Ghaderi et al.), text-fig. 7A.

Holotype: Specimen PIN 1478/42; figured by Shevyrev (1965, pl. 21, fig. 4).

Type locality and horizon: Dorasham 2 (Azerbaijan); *Phisonites triangulus–Iranites transcaucasius* Zone (Late Permian).

Material: Four fragmentary specimens from Aras Valley.

Diagnosis: *Phisonites* with a conch reaching 80 mm dm. Prongs of the external lobe usually multiply serrated; altogether around 25 notches of the E, A and L lobes.

Description: Our material allows only an incomplete description, as all specimens are crushed. Specimen MB.C.22703 is the most complete of these; it has 62 mm in diameter and clearly shows the attenuated umbilical margin and the steep umbilical wall (Fig. 8). Its uw/dm ratio is 0.44.

Discussion: Shevyrev (1965) figured a large and a small fragmentary specimen, the second being the holotype. The three suture lines shown by Shevyrev (1965) are very similar in general outline and number of notches. Though fragmentary, the material allows, because of the characteristic whorl profile, a clear separation from all the other Late Permian ammonoids.

Genus *Iranites* Teichert & Kummel (in Teichert et al. 1973)

Type species: *Tompophiceras transcaucasium* Shevyrev, 1965, by original designation.

Fig. 8. *Phisonites triangulus* Shevyrev, 1965. Specimen MB.C.22703 from the Aras Valley section at −12.90 m. Scale bar units = 1 mm.

Genus diagnosis: Genus of the Xenodiscidae with moderately large conchs (diameter reaching 70 mm). Conch extremely discoidal and evolute, flanks roughly parallel, venter narrowly rounded or acute. Ornament consists of plications, inner whorls with conical nodes.

Included species:

transcaucasius: *Tompophiceras transcaucasium* Shevyrev, 1965; Transcaucasus.

Iranites transcaucasius (Shevyrev, 1965)
Figs. 9, 10

1965 *Tompophiceras transcaucasium* Shevyrev, p. 169, pl. 21, fig. 6.
1968 *Tompophiceras transcaucasium*. – Shevyrev, p. 85, pl. 1, fig. 6.
1973 *Iranites transcaucasius*. – Teichert & Kummel (in Teichert et al.), p. 408, pl. 5, figs. 1–15, text-fig. 11H.
non 1979 *Iranites transcaucasius*. – Bando, p. 132, pl. 5, figs. 8, 10.
2014 *Iranites transcaucasius*. – Korn (in Ghaderi et al.), text-fig. 7B.

Holotype: Specimen PIN 1478/77; figured by Shevyrev (1965, pl. 21, fig. 6).

Type locality and horizon: Dorasham 2 (Azerbaijan); *Phisonites triangulus–Iranites transcaucasius* Zone (Late Permian).

Material: Nine specimens, mostly fragments (Aras Valley: 5; Ali Bashi 4: 3; Ali Bashi 1: 1).

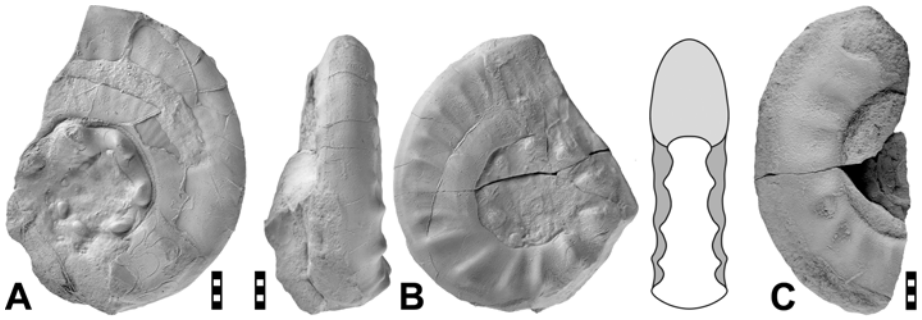

Fig. 9. *Iranites transcaucasius* (Shevyrev, 1965). **A** – Specimen MB.C.29148 from float of the Zal Member in the Aras Valley section. **B** – Specimen MB.C.29149.1 from float of the Zal Member in the Ali Bashi 4 section. **C** – Specimen MB.C.22704 from the Aras Valley section at −13.50 m. Scale bar units = 1 mm.

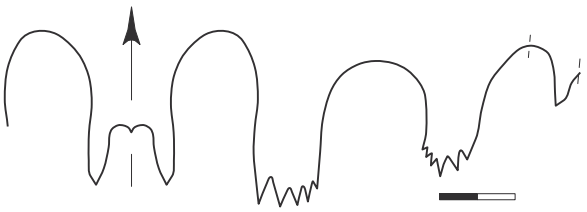

Fig. 10. *Iranites transcaucasius* (Shevyrev, 1965). Suture line of specimen MB.C.29148 from the Aras Valley section, at 8.8 mm ww, 10.3 mm wh. Scale bar units = 1 mm.

Diagnosis: *Iranites* with a conch reaching 70 mm dm. Subadult stage with nearly circular whorl cross section, broadly rounded venter and moderately wide umbilicus (uw/dm ~ 0.40), with coarse conical nodes on the outer flank; adult stage with narrowly rounded or acute venter, with weak lateral plications. Prongs of the external lobe usually simple; altogether about 15 notches of the E, A and L lobes.

Description: The specimens MB.C.29148 and MB.C.29149.1 have 40 and 38 mm diameter, respectively (Fig. 9A, B). While the first has a crushed body chamber, the latter is uncrushed and shows that the conch is extremely discoidal and subevolute (ww/wh = 0.22; uw/dm = 0.38) with a compressed whorl profile (ww/wh = 0.60). The venter is, at 38 mm conch diameter, narrowly rounded and shows an incipient keel. Both specimens show the transformation in the sculpture occurring at about 28 mm diameter; the preadult stage with very coarse conical nodes (8–10 per volution) on the midflank to outer flank changes into the adult stage with elongate, slightly protracting ribs that are coarsest in the ventrolateral area.

The suture line of specimen MB.C.29148 (10 mm whorl height) is characterised by parallel-sided lobes and saddles (Fig. 10); the saddles are inverted U-shaped. The external lobe is nearly as deep as the adventive lobe and possesses unsubdivided prongs. The adventive lobe is flat at its base and shows five small notches and the lateral lobe is weakly rounded with six notches.

Genus *Shevyrevites* Teichert & Kummel (in Teichert et al. 1973)

Type species: *Shevyrevites shevyrevi* Teichert & Kummel (in Teichert et al. 1973), by original designation.

Genus diagnosis: Genus of the family Xenodiscidae with moderately large to large conch, maximum adult diameters are between 60 and 80 mm. Subadult stage with trapezoidal whorl cross section, adult stage variable. Subadult stage with small to large conical ventrolateral nodes, adult stage with weakening sculpture with predominant ribs. Suture line with external lobe that does not reach the depth of the adventive lobe; prongs of the external lobe simple or bifid.

Included species:

shevyrevi: *Shevyrevites shevyrevi* Teichert & Kummel (in Teichert et al. 1973); NW Iran.

nodosus: *Bernhardites nodosus* Shevyrev, 1965; Transcaucasus.

Discussion: Teichert & Kummel (in Teichert et al. 1973) caused some nomenclatorial confusion with their opinion on the species of their new genus *Shevyrevites*. They made clear that "*Celtites radiosus*", the Triassic type species of *Bernhardites* Shevyrev, 1965, differs from the Late Permian forms and that for the latter, a new genus name (*Shevyrevites*) had to be introduced. At the same time, they treated the Transcaucasian material of the two species used by Shevyrev (1965), "*Bernhardites radiosus* Frech (in Noetling 1905)" and "*Bernhardites nodosus* Schevyrev, 1965", as synonyms; they described these under the new genus and species name *Shevyrevites shevyrevi*. This procedure is not acceptable because it suppresses the species name *Shevyrevites nodosus*, which in case of synonymy

of the two species would have priority over *Shevyrevites shevyrevi*. However, this problem is regarded here as minor, as we accept both species as valid.

Shevyrevites shevyrevi Teichert & Kummel (in Teichert et al. 1973)
Figs. 11, 12

1965 *Bernhardites radiosus* Shevyrev, p. 171, pl. 21, figs. 7, 8.
1968 *Bernhardites radiosus*. – Shevyrev, p. 86, pl. 1, fig. 1.
1973 *Shevyrevites shevyrevi* Teichert & Kummel (in Teichert et al.), p. 410, pl. 3, figs. 1–3, 6, text-fig. 11I, K.
non 1978 *Shevyrevites shevyrevi*. – Zhao et al., p. 107, pl. 11, figs. 2–4, 6, 7.
1979 *Shevyrevites shevyrevi*. – Bando, p. 133, pl. 5, figs. 1, 5, pl. 8, figs. 6, 7.

Holotype: Specimen MCZ 9678; illustrated by Teichert & Kummel) in Teichert et al. 1973, pl. 3, figs. 1, 2).

Type locality and horizon: Kuh-e-Ali Bashi (East Azerbaijan, Iran); float from the Ali Bashi Formation (Late Permian), probably *Shevyrevites shevyrevi* Zone.

Material: Three specimens (Aras Valley: 1; Ali Bashi 4: 2).

Diagnosis: *Shevyrevites* with a conch reaching 70 mm dm. Subadult stage with oval, compressed whorl cross section (ww/wh = 0.70–0.90) and rounded venter; 30 coarse ribs per volution. Adult stage with rectangular and compressed whorl cross section (ww/wh = 0.70–0.80), flattened flanks, flattened venter and subangular ventrolateral shoulder; coarse and sharp ribs on the flank, venter smooth. Prongs of the external lobe usually bifid; altogether 20–25 notches of the E, A and L lobes.

Description: Specimen MB.C.29153 is a slightly corroded internal mould and has a conch diameter of 49 mm (Fig. 11A). It is serpenticonic with a compressed whorl profile (ww/wh = 0.74), parallel flanks and a rounded venter. The last volution bears 23 sharp radial ribs, which begin at the umbilical margin and are coarsest and sharpest in the outer flank area, where they diminish. The ribs show variation in their strength; they are most prominent at the end of the phragmocone and beginning of the body chamber (at 35 mm conch diameter). On the body chamber, they decrease markedly in strength. The inner whorls possess only rather faint ribs.

The suture lines of specimen MB.C.29153 and specimen MB.C.29154.1 (both with about 10.5 mm whorl height) have a small external lobe, which reaches only two thirds of the depth of the adventive lobe. Its flanks converge slowly towards the rounded and weakly asymmetric E-A saddle and its prongs are not subdivided. All the three lobes on the flank are intensely serrated with very small notches; there are more than 15 in the A-lobe, nine in the L-lobe and six in the U-lobe. The saddles are broadly rounded; the A-L saddle is rather strongly inflated (Fig. 12A, B).

Fig. 11. *Shevyrevites shevyrevi* Teichert & Kummel, 1973. Specimen MB.C.29153 from float of the Zal Member in the Aras Valley section. Scale bar units = 1 mm.

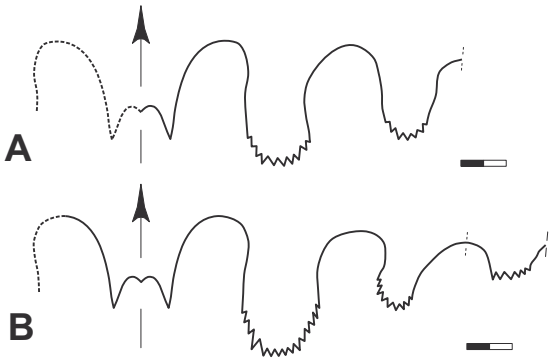

Fig. 12. *Shevyrevites shevyrevi* Teichert & Kummel, 1973 from the Aras Valley section. **A** – Suture line of specimen MB.C.29153, at 8.0 mm ww, 10.6 mm wh. **B** – Suture line of specimen MB.C.29154.1, at 7.0 mm ww, 10.5 mm wh. Scale bar units = 1 mm.

Discussion: *Shevyrevites shevyrevi* differs from *S. nodosus* in the lack of the coarse nodes in the subadult stage.

Shevyrevites nodosus Shevyrev, 1965
Fig. 13

1965 *Bernhardites nodosus* Shevyrev, p. 171, pl. 21, fig. 8.
1968 *Bernhardites nodosus*. – Shevyrev, p. 87, pl. 2, fig. 2.
non 2014 *Shevyrevites nodosus*. – Korn (in Ghaderi et al.), text-fig. 7D. = *Araxoceltites cristatus*.

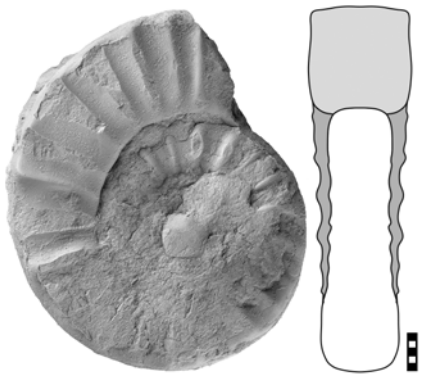

Fig. 13. *Shevyrevites nodosus* (Shevyrev, 1965). Specimen MB.C.29155 from the Aras Valley section at −6.20 m. Scale bar units = 1 mm.

Holotype: Specimen PIN 1478/31; illustrated by Shevyrev (1965, pl. 24, fig. 1).

Type locality and horizon: Ogbin (Armenia); *Shevyrevites shevyrevi* Zone (Late Permian).

Material: One specimen from the Aras Valley section.

Diagnosis: *Shevyrevites* with a conch reaching 80 mm dm. Subadult stage with circular, compressed whorl cross section (ww/wh = 0.60–0.75) and rounded venter; 10 coarse lateral nodes per volution. Adult stage with parallel-sided, slightly compressed whorl cross section (ww/wh = 0.60–0.75), flattened venter and subangular ventrolateral shoulder; radial plications. Prongs of the external lobe simple or bifid; altogether about 15 notches of the E, A and L lobes.

Description: Specimen MB.C.29155 has a conch diameter of 48 mm and allows for the study of a little more than one whorl; the umbilicus is obscured by matrix (Fig. 13B). The conch is subevolute (uw/dm = 0.43) with a slightly compressed rectangular whorl profile (ww/wh = 0.74) and has a flattened venter. The specimen possesses sharp ribs of equal strength on the last one and a quarter volutions. These ribs are weakly sinuous on the last volution; they begin at the umbilical margin and become coarsest in the ventrolateral area, where they end abruptly. On the penultimate volution, the ribs are coarsest in the midflank area.

Discussion: *Shevyrevites nodosus* differs from *S. shevyrevi* in the presence of coarse nodes in the subadult stage.

Genus *Araxoceltites* nov.

Etymology: From the Araxes (= Aras) Valley and the attribution to the Paraceltitina.

Type species: *Araxoceltites sanestepanus* sp. nov.

Genus diagnosis: Genus of the family Xenodiscidae with moderately large to large conch; maximum adult diameters reaching 100 mm. Subadult stage with circular or oval whorl cross section, adult stage with parallel or converging flanks, umbilical margin may be attenuated. Subadult stage with small to large conical ventrolateral nodes or simple ribs, adult stage with ribs and sharp elongate nodes on the midflank and ventrolateral shoulder. Suture line with broad external lobe that does not reach the depth of the adventive lobe, flanks of the external lobe rapidly diverging; prongs of the external lobe bifid to multiply serrated.

Included species:

cristatus: *Araxoceltites cristatus* n. sp.; NW Iran.

sanestepanus: *Araxoceltites sanestepanus* n. sp.; NW Iran.

laterocostatus: *Araxoceltites laterocostatus* n. sp.; NW Iran.

Discussion: *Araxoceltites* differs from most of the other genera of the family Xenodiscidae in the coarse sculpture. *Iranites* and *Shevyrevites* have also a coarse sculpture, but differ in the simple ribs, while *Araxoceltites* possesses ribs that are strengthened in the midflank and the ventrolateral areas. Furthermore, both genera have a much narrower external lobe when compared with *Araxoceltites*.

Araxoceltites sanestepanus sp. nov.
Figs. 14, 15

Etymology: After the nearby historical Armenian Saint Stepanos monastery, UNESCO world heritage site.

Holotype: Specimen MB.C.29156, illustrated in Fig. 14A.

Type locality and horizon: Aras Valley section (West Azerbaijan, Iran); Zal Member, 9.50 m below the extinction horizon.

Diagnosis: *Araxoceltites* with a conch reaching 100 mm dm. Adult stage extremely discoidal and subevolute (ww/dm ~ 0.20; uw/dm ~ 0.40), with weakly trapezoidal, compressed whorl cross section (ww/wh ~ 0.60) and flattened venter; numerous sharp ribs. Ribs in the preadult stage form sharp elongate nodes in the midflank and ventrolateral area. Prongs of the external lobe multiply serrated; altogether 17 to 21 notches of the E, A and L lobes.

Material: Thirteen fragmentary specimens (Aras Valley: 10; Ali Bashi N: 1; Zal: 2).

Description: Holotype MB.C.29156 is, though fragmentary preserved, the best of the available specimens (Fig. 14A). It has 88 mm conch diameter, but only half of a volution of the body chamber can be studied. It is extremely discoidal (ww/dm = 0.18) and subevolute (uw/dm = 0.39). The whorl profile is weakly trapezoidal and widest at the subangular ventrolateral shoulder; the venter is flattened, the flanks are slightly concave and the umbilical margin is broadly

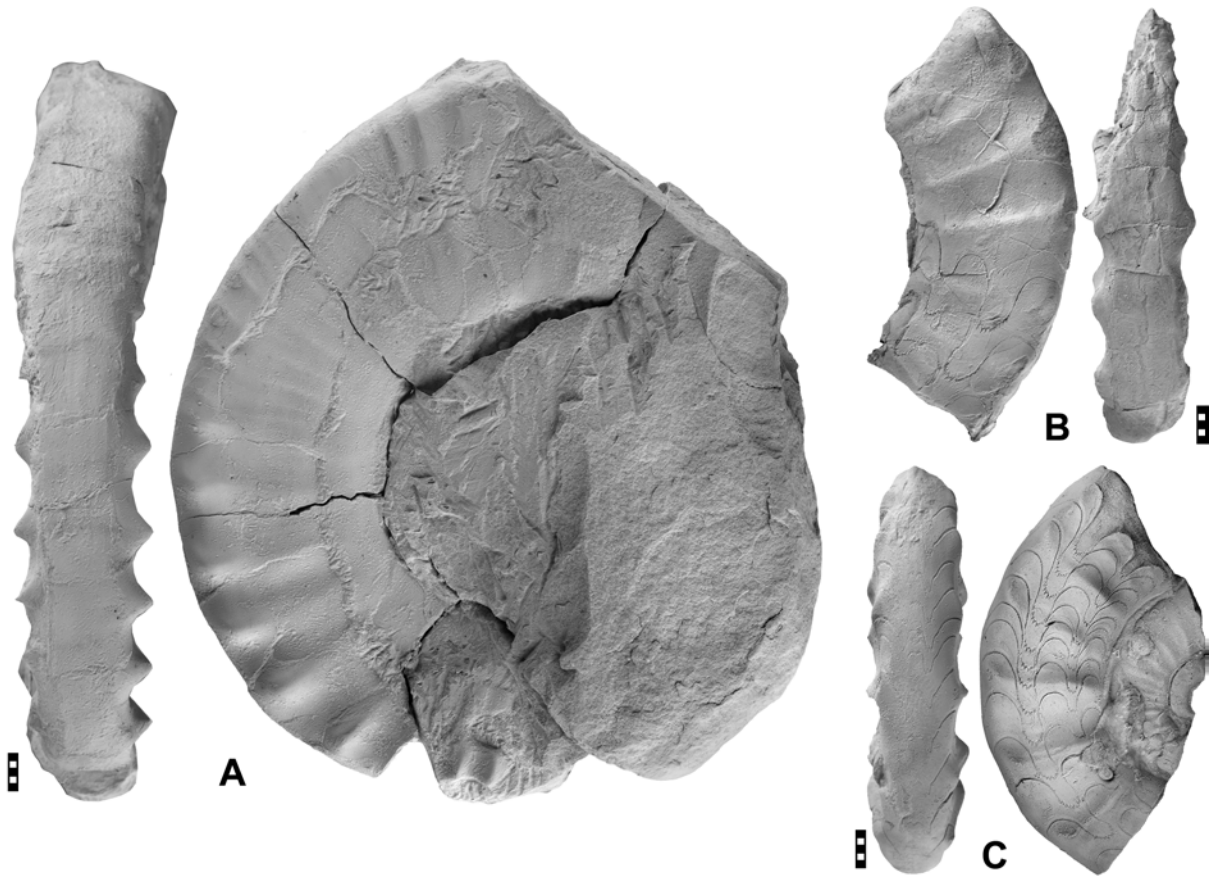

Fig. 14. *Araxoceltites sanestapanus* n. sp. **A** – Holotype MB.C.29156 from the Aras Valley section at −9.50 m. **B** – Paratype MB.C.29158 from the Aras Valley section at −11.60 m. **C** – Paratype MB.C.29157 from float of the Zal Member in the Aras Valley section. Scale bar units = 1 mm.

rounded to form a very shallow umbilical wall. On the segment consisting only one half of a whorl, there is a conspicuous weakening of the sculpture observable. At the beginning, there are radial ribs that possess prominent elongate nodes in the midflank and short nodes on the ventrolateral shoulder. Only the latter maintain throughout the half volution, but they become much weaker and more densely spaced.

Paratypes MB.C.29158 and MB.C.29157 show very similar shape and sculpture details (Fig. 14B, C). It appears that they show coarser ribs than the holotype. Paratype MB.C.29157 allows insight in the weakly ribbed penultimate volution and the smooth volution before, demonstrating the ontogenetic sculpture change towards coarser sculpture in a later growth stage.

The suture lines of paratypes MB.C.29157 (17 mm wh) and MB.C.29158 (21.5 mm wh) show a Y-shaped external lobe with rapidly diverging, sinuous flanks. While the external lobe is much narrower at its base in specimen MB.C.29158, it appears rather wide in specimen MB.C.29157; the prongs possess three or four notches. The adventive lobe is U-shaped and weakly asymmetric with semicircular base with nine or eleven small notches; the lateral lobe has slowly diverging flanks in both specimens with five or six notches (Fig. 15D, E).

Discussion: *Araxoceltites sanestepanus* differs from *A. laterocostatus* in the more compressed conch (ww/wh ~ 0.60 in *A. sanestapanus*, but 0.70–0.75 in *A. laterocostatus*). More important, *A. sanestapanus* lacks the coarse conical nodes of the preadult stage.

Araxoceltites laterocostatus n. sp.
Figs. 16, 17

2014 *Dzhulfites nodosus*. – Korn (in Ghaderi et al.), textfig. 7C.

Etymology: Named after the ribs in the midflank area.

Holotype: Specimen MB.C.29164, illustrated in Fig. 16A.

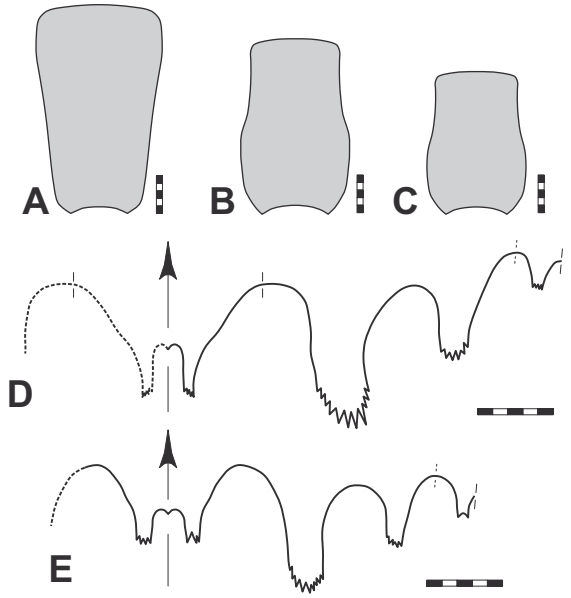

Fig. 15. *Araxoceltites sanestapanus* n. sp. from the Aras Valley section. **A** – Whorl profile of holotype MB.C.29156. **B** – Whorl profile of paratype MB.C.29158. **C** – Whorl profile of paratype MB.C.29157. **D** – Suture line (reversed) of paratype MB.C.29158, at 13.6 mm ww, 21.4 mm wh. **E** – Suture line of paratype MB.C.29157, at 11.2 mm ww, 17.7 mm wh. Scale bar units = 1 mm.

Type locality and horizon: Aras Valley section (West Azerbaijan, Iran); float from the Zal Member.

Material: Two fragmentary specimens from Aras Valley.

Diagnosis: *Araxoceltites* with a conch reaching 100 mm dm. Adult stage extremely discoidal and subevolute (ww/dm ~ 0.25; uw/dm ~ 0.40), with weakly subttrapezoidal, compressed whorl cross section (ww/wh = 0.70–0.75) and flat venter; numerous sharp ribs. Ribs in the preadult stage form sharp elongate nodes in the midflank and ventrolateral area. Prongs of the external lobe multiply serrated; altogether 17 to 26 notches of the E, A and L lobes.

Description: Both the holotype MB.C.29164 and the paratype MB.C.22705 are whorl fragments with about 22 mm whorl height. The partly crushed holotype consists of a portion of the body chamber, a portion of the phragmocone and part of the penultimate volution (Fig. 16A). The specimen shows that the conch was subevolute. The compressed whorl profile (ww/wh = 0.74) is subtrapezoidal and widest in the midflank area; from here the flanks converge towards the broadly rounded umbilical wall and towards the angular ventrolateral shoulder. The venter is nearly flat.

There occurs a conspicuous transformation in the sculpture from the penultimate to the last volution. While there are very prominent conical nodes present in the preadult stage, the sculpture of the last whorl consists of coarse radial ribs with pronounced elongate nodes in the midflank area and rounded nodes on the ventrolateral shoulder. On the body chamber, these nodes become markedly weaker.

Paratype MB.C.22705 compliments the holotype in shape and sculpture, but only a fully chambered portion of one volution is preserved. It shows the sculpture stage with weakened ribs on the flank, which give rise to sharp elongate nodes on the middle of the flank and the ventrolateral shoulder (Fig. 16B).

The suture lines of the two specimens MB.C.29164 (20 mm wh) and MB.C.22705 (23 mm wh) are rather similar in their general outline but differ in some details, particularly in the number of notches in the lobes (Fig. 17C, D). Both have a wide external lobe that reaches the depth of only two thirds of the adventive lobe depth and possess rapidly diverging, incurved flanks. The prongs may be asymmetric with respect to the size of the notches, of which both specimens show four in each prong. The adventive lobe is U-shaped in both specimens and strongly serrated at the base with nine (MB.C.29164) or 14 (MB.C.22705) notches. Differences in the number of notches occur also in the lateral lobes (four in specimen MB.C.29164, eight in specimen MB.C.22705), which show slowly diverging flanks in both specimens.

Discussion: *Araxoceltites laterocostatus* differs from *A. sanestapanus* in the wider conch (ww/wh ~ 0.70 in *A. laterocostatus*, but only ~ 0.60 in *A. sanestapanus*) and in the presence of coarse conical nodes of the preadult stage.

Araxoceltites cristatus n. sp.
Figs. 18, 19

2014 *Shevyrevites nodosus*. – Korn (in Ghaderi et al.), text-fig. 7D.

Etymology: From Latin cristatus = ridge, because of the shape of the umbilicus.

Holotype: Specimen MB.C.22706, illustrated in Fig. 18C.

Type locality and horizon: Aras Valley section (West Azerbaijan, Iran); Zal Member, 6.20 m below the extinction horizon.

Material: 37 specimens of which all but the holotype are fragmentary (Aras Valley: 16; Ali Bashi 4: 5; Zal: 16).

Diagnosis: *Araxoceltites* with a conch reaching 90 mm dm. Subadult stage with subtrapezoidal, weakly compressed whorl cross section (ww/wh ~ 0.75), weakly attenuated umbilical margin and broadly rounded venter; 10 coarse conical lateral nodes per volution. Adult stage with subtrapezoidal and weakly compressed whorl cross section, with raised umbilical margin, concave flanks, angular ventrolateral shoulder and flat venter; densely spaced radial riblets. Prongs of the external lobe bifid; altogether about 19 notches of the E, A and L lobes.

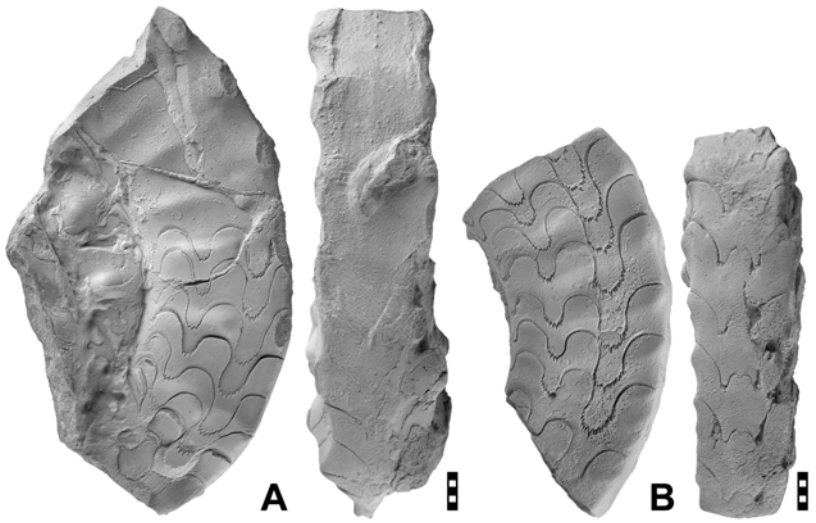

Fig. 16. *Araxoceltites laterocostatus* n. sp. **A** – Holotype MB.C.29164 from float of the Zal Member in the Aras Valley section. **B** – Paratype MB.C.22705 from float of the Zal Member in the Aras Valley section. Scale bar units = 1 mm.

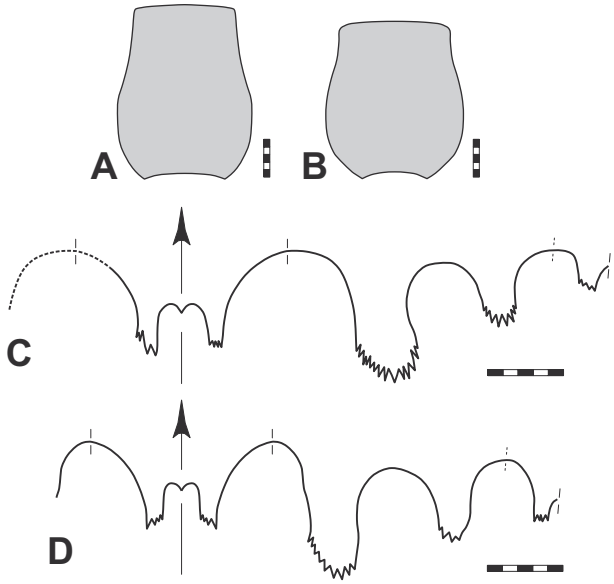

Fig. 17. *Araxoceltites laterocostatus* n. sp. from the Aras Valley section. **A** – Whorl profile of paratype MB.C.22705. **B** – Whorl profile of holotype MB.C.29164. **C** –Suture line (reversed) of paratype MB.C.22705, at 16.5 mm ww, 23.0 mm wh. **D** – Suture line of holotype MB.C.29164, at 15.8 mm ww, 19.0 mm wh. Scale bar units = 1 mm.

Description: Holotype MB.C.22706 is the only rather completely preserved specimen; it has 46 mm conch diameter and allows the study of about one and a half whorls of which the last half whorl belongs to the body chamber (Fig. 18C). The conch is thinly discoidal and subevolute (ww/dm = 0.26; uw/dm = 0.42) and the whorl profile is compressed (ww/wh = 0.77). It is widest at the weakly raised umbilical margin, from where the flanks converge slightly incurved towards the subangular ventrolateral shoulder that separated the broadly arched venter. The sculpture changes markedly from being dominated by rather sharp elongate nodes on the midflank to an ornament consisting of rather sharp sinuous ribs that are most pronounced on the inner flank and form elongate ventrolateral nodes.

Larger specimens such as paratype MB.C.29165.1 (24 mm whorl height) show then a much higher raised umbilical ridge, a more angular ventrolateral shoulder and a flat venter (Figs. 18A, 19B). The sculpture is weaker and consists of densely spaced riblets on the flank.

The suture lines of the two paratypes MB.C.29166.1 (14 mm wh) and MB.C.29167.1 (14.5 mm wh) are similar in their general outline (Fig. 19C, D). There are only minor differences in the shape of lobes and saddles and the number of lobe notches. The external lobe is broadly V-shaped with rapidly diverging, slightly concave flanks and bifid prongs. Both the adventive and lateral lobes are U-shaped with numerous notches of the adventive (9–11) and lateral (6–8) lobe. The E-A saddle is asymmetric and parabolic in its shape and the A-L saddle is turned U-shaped.

Discussion: *Araxoceltites cristatus* differs from the other two species of the genus in the conspicuously raised umbilical margin. A superficially similar species is *Phisonites triangulus*, but this has a subacute venter.

Family Dzhulfitidae Shevyrev, 1965

Included genera: *Dzhulfites* Shevyrev, 1965; *Paratirolites* Stoyanow, 1910; *Julfotirolites* Korn & Ghaderi (in Korn et al. 2016); *Alibashites* Korn & Ghaderi (in Korn et al. 2016); *Abichites* Shevyrev, 1965; *Stoyanowites* Korn (in Ghaderi et al. 2014).

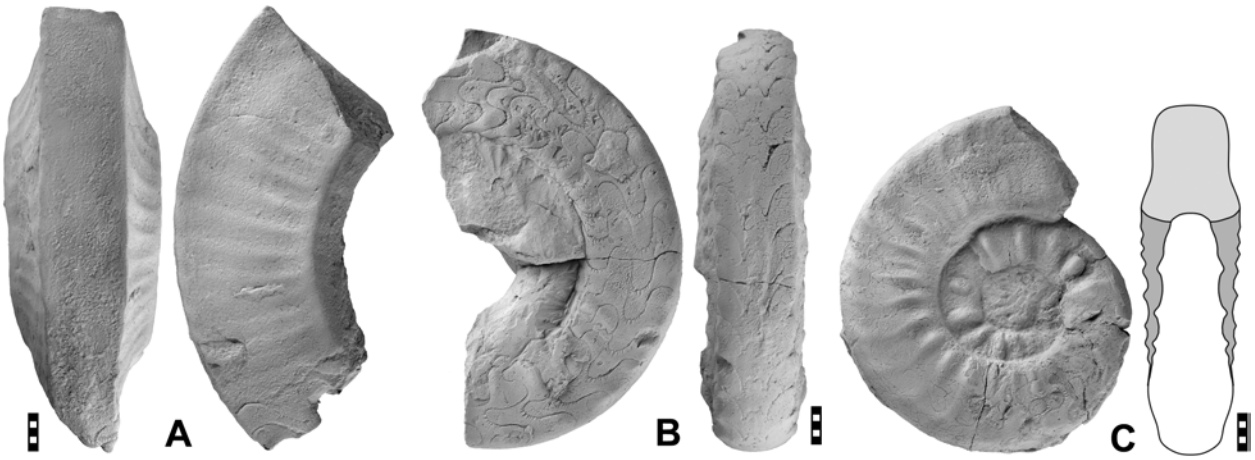

Fig. 18. *Araxoceltites cristatus* n. sp. **A** – Paratype MB.C.29165.1 from float of the Zal Member in the Aras Valley section. **B** – Paratype MB.C.29167.1 from float of the Zal Member in the Aras Valley section. **C** – Holotype MB.C.22706 from float of the Zal Member in the Aras Valley section. Scale bar units = 1 mm.

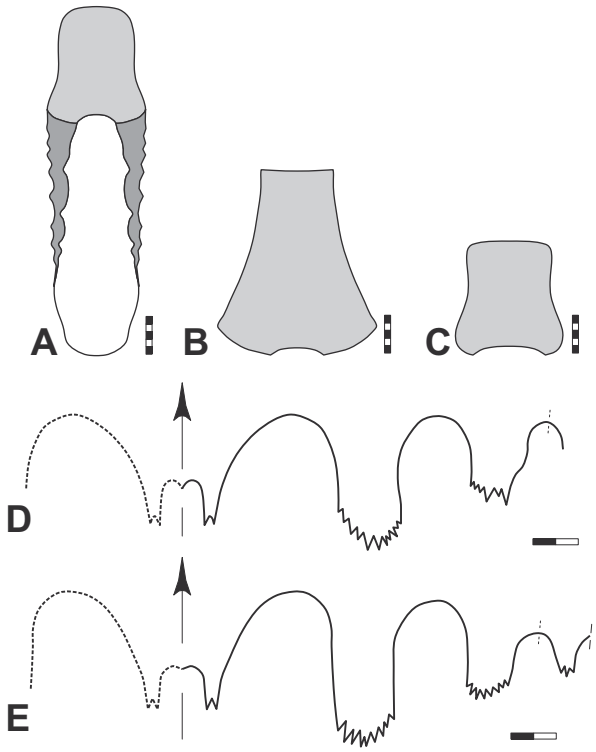

Fig. 19. *Araxoceltites cristatus* n. sp. **A** – Whorl profile of paratype MB.C.29165.1 from the Aras Valley section. **B** – Whorl profile of paratype MB.C.29167.1 from the Aras Valley section. **C** – Suture line of paratype MB.C.29167.1 from the Aras Valley section, at 12.4 mm ww, 14.6 mm wh. **D** – Suture line (reversed) of paratype MB.C.29166.1 from the Ali Bashi 4 section, at 10.6 mm ww, 14.0 mm wh. Scale bar units = 1 mm.

Genus *Dzhulfites* Shevyrev, 1965

Type species: *Dzhulfites spinosus* Shevyrev, 1965, by original designation.

Genus diagnosis: Representatives of the family Dzhulfitidae with moderately large to large conch; maximum adult diameters are between 80 and 120 mm. Subadult stage with trapezoidal whorl cross section, adult stage variable. Subadult stage with small to large conical ventrolateral nodes, adult stage with weakening sculpture. Suture line with external lobe that does not reach the depth of the adventive lobe; prongs of the external lobe simple or bifid.

Included species:

spinosus: *Dzhulfites spinosus* Shevyrev, 1965; Transcaucasus.

nodosus: *Dzhulfites nodosus* Shevyrev, 1965; Transcaucasus.

zalensis: *Dzhulfites zalensis* Korn & Ghaderi (in Korn et al. 2016); NW Iran.

hebes: *Dzhulfites hebes* Korn & Ghaderi (in Korn et al. 2016); NW Iran.

Dzhulfites spinosus Shevyrev, 1965
Figs. 20, 21

1965 *Dzhulfites spinosus* Shevyrev, p. 173, pl. 21, fig. 9, pl. 22, fig. 1.

1968 *Dzhulfites spinosus*. – Shevyrev, p. 88, pl. 2, figs. 3, 4.

non 1973 *Paratirolites spinosus*. – Teichert & Kummel (in Teichert et al.), p. 413, pl. 6, figs. 2, 6, pl. 7, figs. 4, 5, 10, 11. (= possibly various species of *Paratirolites*)

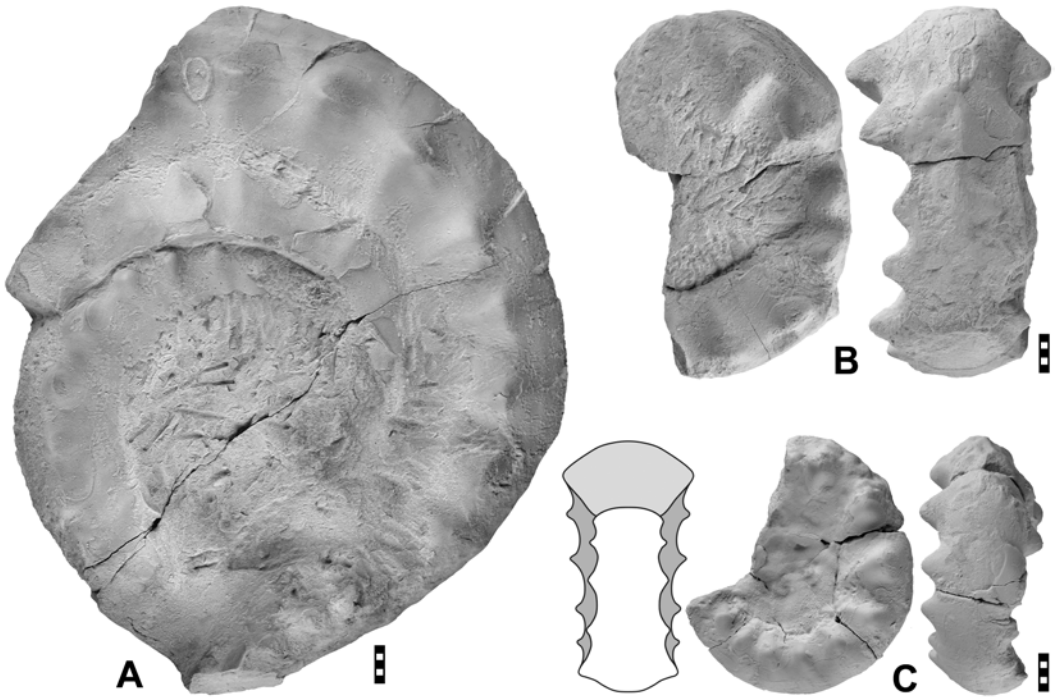

Fig. 20. *Dzhulfites spinosus* Shevyrev, 1965. **A** – Specimen MB.C.29177 from the Aras Valley section at −7.60 m. **B** – Specimen MB.C.25174 from float of the Zal Member in the Aras Valley section. **C** – Specimen MB.C.29178 from the Aras Valley section at −9.50 m. Scale bar units = 1 mm.

non 1979 *Paratirolites spinosus*. – Bando, p. 136, pl. 5, fig. 11, pl. 6, figs. 4, 5. (= possibly various species of *Paratirolites* and related genera)

2016 *Dzhulfites spinosus*. – Korn & Ghaderi (in Korn et al.), text-figs. 3B, 13A, B.

Holotype: Specimen PIN 1478/60; figured by Shevyrev (1965, pl. 21, fig. 9).

Type locality and horizon: Dorasham 2 (Azerbaijan); *Dzhulfites nodosus* Zone (Late Permian).

Material: Seven fragmentary specimens (Aras Valley: 5; Zal: 2).

Diagnosis: *Dzhulfites* with a conch reaching 80 mm dm. Subadult and adult stage with trapezoidal, moderately depressed whorl cross section (ww/wh ~ 1.60) and broadly rounded venter; about 12 coarse conical lateral nodes per volution. Prongs of the external lobe simple or bifid; altogether about 16 notches of the E, A and L lobes.

Description: Specimen MB.C.29178 is an example of the preadult stage (Fig. 20C). It has 31 mm diameter and a discoidal shape with wide umbilicus (ww/dm = 0.46; uw/dm = 0.46) and a moderately depressed whorl profile (ww/wh = 1.60, measured at the nodes) with broadly rounded venter. The coarse sculpture consists of conical nodes on the outer flank; there are about 12 such nodes on one volution.

The larger fragment MB.C.25174 (48 mm diameter) has a similar shape, but its nodes are more pronounced and form rather prominent spines (Fig. 20B). They originate from lateral ribs, which begin in the midflank.

Three suture lines could be studied, they are of specimens with 7 mm wh (MB.C.29178), 10 mm wh (J2013-018) and 15 mm wh (MB.C.25174). These suture lines show some similarities but also differences; the external lobe, for instance, has a similar shape in all of them, being wider in the lower half and constricted in the upper half (Fig. 21A–C). The prongs are usually unsubdivided, but specimen MB.C.25174 shows an asymmetry with a bifid prong on one side (Fig. 21A). On the venter follow an inflated, narrowly or broadly rounded E-A saddle and then, on the ventrolateral shoulder, an asymmetric adventive lobe with numerous notches. The A-L saddle is inverted U-shaped and rather broad; the lateral lobe is parallel-sided with five irregular notches in specimen J2013-018 (Fig. 21B).

Discussion: *Dzhulfites spinosus* differs from the other species of *Dzhulfites* in the very broad convex shape of the venter. A similar species is *D. hebes*, but this possesses a much slenderer conch (ww/wh = 1.60 in *D. spinosus* but only 1.10 in *D. hebes*).

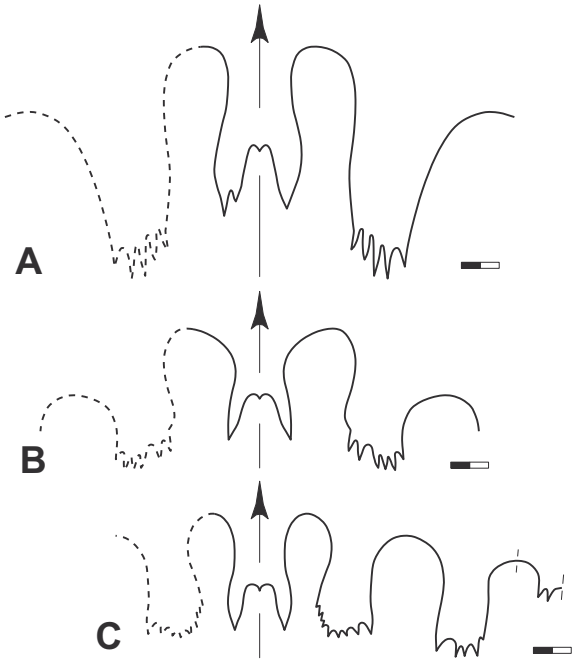

Fig. 21. *Dzhulfites spinosus* Shevyrev, 1965; suture lines from specimens from the Aras Valley section. **A** – Specimen MB.C.25174 (reversed), at 25.5 mm ww, 15.2 mm wh. **B** – Specimen MB.C.22706 from the Aras Valley section, at 27.5 mm ww, 10.0 mm wh. **C** – Specimen MB.C.29178 (reversed) , at 23.5 mm dm, 9.5 mm ww, 6.8 mm wh. Scale bar units = 1 mm.

Dzhulfites nodosus Shevyrev, 1965
Figs. 22, 23

1965 *Dzhulfites nodosus* Shevyrev, p. 174, pl. 22, figs. 2, 3.
1968 *Dzhulfites nodosus*. – Shevyrev, p. 89, pl. 2, fig. 5, pl. 3, fig. 4.
non 2014 *Dzhulfites nodosus*. – Korn (in Ghaderi et al.), text-fig. 7C.

Holotype: Specimen PIN 1478/59; figured by Shevyrev (1965, pl. 22, fig. 3).

Type locality and horizon: Dorasham 2 (Azerbaijan); *Dzhulfites nodosus* Zone (Late Permian).

Material: Twenty-three fragmentary specimens (Aras Valley: 13; Ali Bashi 4: 2; Zal: 8).

Diagnosis: *Dzhulfites* with a conch reaching 120 mm dm. Subadult stage with oval, weakly depressed whorl cross section (ww/wh ~ 1.35) and broadly rounded venter; 10 coarse conical lateral nodes per volution. Adult stage with trapezoidal and weakly depressed whorl cross section (ww/wh ~ 1.05), flat venter and angular ventrolateral shoulder; about 15 coarse ventrolateral nodes. Prongs of the external lobe simple or bifid; altogether about 10–12 notches of the E, A and L lobes.

Description: Specimen MB.C.29182 is, though fragmentarily preserved, the best of the available material (Fig. 22A). It is fully chambered at a diameter of 97 mm, where it is extremely discoidal and subevolute (ww/dm = 0.26; uw/dm = 0.42) with a trapezoidal, compressed whorl profile (ww/wh = 0.82). The flanks are sinuous in section with a broadly rounded umbilical margin and an oblique umbilical wall, the ventrolateral shoulder is narrowly rounded; the venter is broadly rounded at the beginning of the last preserved volution but flat at the end. The ornament shows a change from the presence of eight shallow flank ribs ending in prominent ventrolateral nodes at the penultimate quarter of whorls towards more densely spaced weaker plications and nodes in the last quarter whorl.

The suture line of specimen MB.C.29182 shows elongate elements with nearly straight and parallel-arranged flanks of lobes and saddles (Fig. 23). The external lobe is nearly twice as deep as wide; it possesses bifid prongs and reaches the depth of the adventive lobe. Both lobes are separated by an inverted U-shaped saddle. The very narrow and trifid adventive lobe (the depth is 2.5 times of the width) has a position on the side of the venter; the A-L saddle is asymmetric because it is influenced by the coarse ventrolateral nodes. The flanks are occupied by the large, weakly V-shaped lateral lobe with four rather large notches; it is followed on the inner flank by the very asymmetric, dorsally inclined L-U saddle and a bifid umbilical lobe.

Discussion: *Dzhulfites nodosus* differs from *D. spinosus* and *D. hebes* in the flat venter. Another species of *Dzulfites* with flat venter is *D. zalensis*, but this differs in the much wider whorl profile and the coarser ribs from *D. nodosus*.

Possibly reworked material

Vedioceras sp.
Figs. 24A, 25

Specimen MB.C.29195 from the base of the Zal Member in the Ali Bashi 1 section is a segment of a specimen with 25 mm whorl height. It is fully chambered and shows a raised umbilical ridge, concave flanks, a subangular ventrolateral shoulder and a flattened venter. Only a part of the suture line is visible. It shows a rather large adventive lobe located on outer flank and venter; it possesses large denticles. Denticulation of the lateral lobe is very asymmetric with a large denticle on the dorsal side (Fig. 25).

Dzhulfoceras sp.
Figs. 24B

The single specimen MB.C.29196 from the upper part of the Zal Member has a diameter of 24 mm with part of the body chamber preserved. It is discoidal with a weakly raised

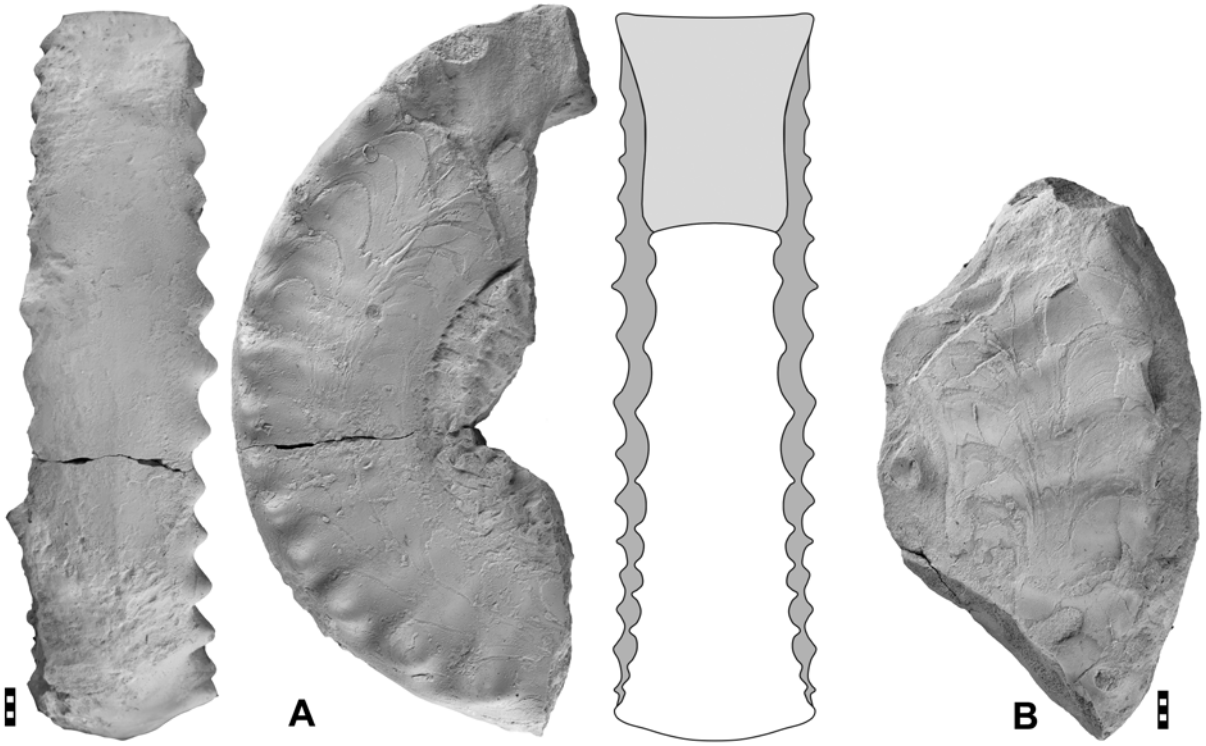

Fig. 22. *Dzhulfites nodosus* Shevyrev, 1965. **A** – Specimen MB.C.29182 from the Aras Valley section at −9.50 m. **B** – Specimen MB.C.29183 from float of the Zal Member in the Aras Valley section. Scale bar units = 1 mm.

Fig. 23. *Dzhulfites nodosus* Shevyrev, 1965. Suture line of specimen MB.C.29182, at 21.0 mm ww, 22.5 mm wh. Scale bar units = 1 mm.

umbilical margin, a subangular margin and a rounded venter. Septal crowding at the end of the phragmocone may be an indication of adulthood. The suture line is corroded but shows that the adventive lobe with numerous small denticles has a position on the outer flank.

Acknowledgements

We gratefully acknowledge the Aras Free Zone Office (Julfa) for supporting our field sessions. We also acknowledge the careful mechanical preparation of the material by Evelyn Stenzel and Markus Brinkmann (Berlin) as well as Jenny Huang and Jamie Lembke

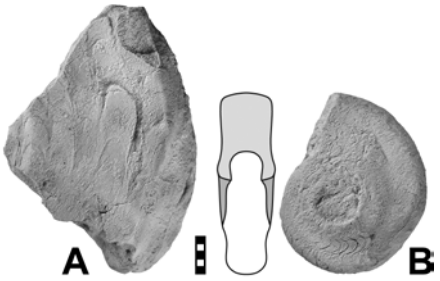

Fig. 24. A –*Vedioceras* sp. Specimen MB.C.29195 from the Ali Bashi 1 section at −15.80 m. **B** –*Dzhulfoceras* sp. Specimen MB.C.29196 from the Ali Bashi 1 section at −5.20 m. Scale bar units = 1 mm.

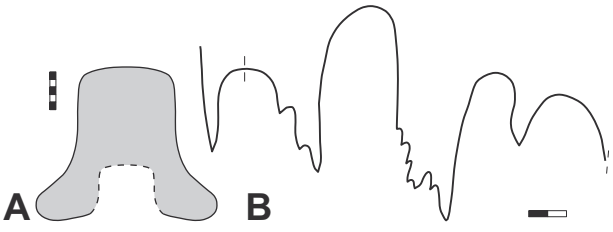

Fig. 25. *Vedioceras* sp., specimen MB.C.29195 from the Ali Bashi 1 section at −15.80 m. A – Whorl profile. B – Suture line at 24 mm wh. Scale bar units = 1 mm.

(Berlin) for taking photographs. The project was supported by the Deutsche Forschungsgemeinschaft (DFG projects Ko1829/12–1, Ko1829/18–1 and FOR2332) and the National Natural Science Foundation of China (grant nr. 41630101). NGT was funded by the Ferdowsi University of Mashhad (grant nr. 3/45510). We acknowledge the review of the manuscript by Arnaud Brayard (Dijon) and Dai Xu (Wuhan).

References

Arakelyan, R.A., Grunt, T.A., & Shevyrev, A.A. (1965). Kratkiy stratigraficheskiy ocherk. – In V.E. Ruzhencev, & T.G. Sarytcheva, Rasvitie i smena morskikh organizmov na rubezhe Paleozoya i Mezozoya. Trudy Paleontologicheskogo Instituta Akademiya Nauk SSSR, **108**, 20–25.

Bando, Y. (1979). Upper Permian and Lower Triassic ammonoids from Abadeh, Central Iran. Memoirs of the Faculty of Education. Kagawa University, **29**, 103–138.

Frech, F. (1897–1902). Lethaea geognostica oder Beschreibung und Abbildung der für die Gebirgs-Formationen bezeichnendsten Versteinerungen. I. Theil. Lethaea palaeozoica. 2. Band.

Furnish, W.M. (1966). Ammonoids of the Upper Permian *Cyclolobus*-Zone. Neues Jahrbuch für Geologie und Paläontologie, Abhandlungen, **125**, 265–296.

Ghaderi, A. (2014). Stratigraphy and paleoecology of the Upper Permian to Permian – Triassic boundary in the northwest of Iran based on biostratigraphic data of conodonts and brachiopods. Mashhad: Ferdowsi University of Mashhad.

Ghaderi, A., Garbelli, C., Angiolini, L., Ashouri, A.R., Korn, D., Rettori, R., & Gharaie, M.H.M. (2014a). Faunal change near the end-Permian extinction: The brachiopods of the Ali Bashi Mountains, NW Iran. Rivista Italiana di Paleontologia e Stratigrafia, **120**, 27–59.

Ghaderi, A., Leda, L., Schobben, M., Korn, D., & Ashouri, A.R. (2014b). High-resolution stratigraphy of the Changhsingian (Late Permian) successions of NW Iran and the Transcaucasus based on lithological features, conodonts, and ammonoids. Fossil Record, **17**(1), 41–57. doi: 10.5194/fr-17-41-2014

Haniel, C.A. (1915). Die Cephalopoden der Dyas von Timor. In J. Wanner (ed.), Paläontologie von Timor, 3(6), 1–153.

Hyatt, A. (1883–1884). Genera of fossil cephalopods. Proceedings of the Boston Society of Natural History, **22**, 253–338.

Hyatt, A. (1900). Tetrabranchiate Cephalopoda. In K.A. Zittel, v. & C.R. Eastman (eds.), Text-book of palaeontology, volume 1, 1st edition. London: Macmillan and Company: 502–604.

Isaa, A., Ghaderi, A., Ashouri, A.R., & Korn, D. (2016). Late Permian – Early Triassic conodonts of the Zal section at the northwest of Iran. Stratigraphy and Sedimentology Researches, **32**, 55–74.

Kiessling, W., Schobben, M., Ghaderi, A., Hairapetian, V., Leda, L., & Korn, D. (2018). Pre–mass extinction decline of latest Permian ammonoids. Geology, **46**(3), 283–286. doi: 10.1130/G39866.1

Korn, D. (2010). A key for the description of Palaeozoic ammonoids. Fossil Record, **13**(1), 5–12. doi: 10.1002/mmng.200900008

Korn, D., Ebbighausen, V., Bockwinkel, J., & Klug, C. (2003). The A-mode sutural ontogeny in prolecanitid ammonoids. Palaeontology, **46**(6), 1123–1132. doi: 10.1046/j.0031-0239.2003.00336.x

Korn, D., Ghaderi, A., Leda, L., Schobben, M., & Ashouri, A.R. (2016). The ammonoids from the Late Permian *Paratirolites* Limestone of Julfa (East Azerbaijan, Iran). Journal of Systematic Palaeontology, **14**(10), 841–890. doi: 10.1080/14772019.2015.1119211

Kotlyar, G.V., Zakharov, Y.D., Koczyrkevich, B.V., Kropatcheva, G.S., Rostovtsev, K.O., Chedia, I.O., Vuks, G.P., & Guseva, E.A. (1983). Dzhul'finskiy i Dorashamskiy yarusy SSSR. In M.N. Gramm & K.O. Rostovtsev (eds.), Pozdnepermskiy etap evolyutsii organicheskogo mira: 1–190.

Kummel, B. (1972). The Lower Triassic (Scythian) Ammonoid *Octoceras*. Bulletin of the Museum of Comparative Zoology, Harvard University, **143**, 365–417.

Leda, L., Korn, D., Ghaderi, A., Hairapetian, V., Struck, U., & Reimold, W.U. (2014). Lithostratigraphy and carbonate microfacies across the Permian–Triassic boundary near Julfa (NW Iran) and in the Baghuk Mountains (Central Iran). Facies, **60**(1), 295–325. doi: 10.1007/s10347-013-0366-0

Leonova, T.B. (2002). Permian Ammonoids: Classification and Phylogeny. Paleontological Journal, Supplements, **36**, 1–114.

Miller, A.K., & Furnish, W.M. (1940). Geological Society of America, Special Papers: **Vol. 26**. Permian ammonoids of the Guadalupe Mountain Region and adjacent areas (pp. 1–242). doi: 10.1130/SPE26-p1

Noetling, F. (1905). Lethaea geognostica, Teil 2: Lethaea mesozoica: Die asiatische Trias: 107–221.

Ruzhencev, V.E. (1951). Nizhnepermskie ammonity yuzhnogo Urala. 1. Ammonity Sakmarskogo Yarusa. Trudy Paleontologicheskogo Instituta Akademiya Nauk SSSR, **33**, 1–186.

Ruzhencev, V.E. (1952). Biostratigrafiya Sakmarskogo Yarusa v Aktyubinskoy Oblasti Kazakhskoy SSR. Trudy Paleontologicheskogo Instituta Akademiya Nauk SSSR, **42**, 1–85.

Ruzhencev, V.E. (1956). Nizhnepermskiye ammonity Yuzhnogo Urala. II. Ammonity Artinskogo yarusa. Trudy Paleontologicheskogo Instituta Akademiya Nauk SSSR, **60**, 1–271.

Ruzhencev, V.E. (1962). Klassifikatsia semeystve Araxoceratidae. Paleontologicheskiy Zhurnal, **1962**, 88–103.

Ruzhencev, V.E. (1963). Novye dannye o semeystve Araxoceratidae. Paleontologicheskiy Zhurnal, **1963**, 56–64.

Ruzhencev, V.E., Sarytcheva, T.G., & Shevyrev, A.A. (1965). Biostratigraficheskie vyvody. In V.E. Ruzhencev & T.G. Sarytcheva (eds.), Rasvitie i smena morskikh organizmov na rubezhe Paleozoya i Mezo-

zoya. Trudy Paleontologicheskogo Instituta Akademiya Nauk SSSR, 108, 93–116.

Ruzhencev, V.E., & Shevyrev, A.A. (1965). Ammonoidei. In V.E. Ruzhencev & T.G. Sarytcheva (eds.), Razvitie i smena morskikh organizmov na rubezhe Paleozoya i Mezozoya. Trudy Paleontologicheskogo Instituta Akademiya Nauk SSSR, 108, 47–57.

Schindewolf, O.H. (1929). Vergleichende Studien zur Phylogenie, Morphologie und Terminologie der Ammoneen-Lobenlinie. Abhandlungen der Preußischen Geologischen Landesanstalt, Neue Folge, **115**, 1–102.

Schobben, M., Heuer, F., Tietje, M., Ghaderi, A., Korn, D., Korte, C., & Wignall, P.B. (2019). Chemostratigraphy Across the Permian-Triassic Boundary: The Effect of Sampling Strategies on Carbonate Carbon Isotope Stratigraphic Markers. In A.N. Sial, C. Gaucher, R. Muthuvairavasamy, & P.F. Valderez (eds.), Geophysical Monograph: **Vol. 240**. Chemostratigraphy Across Major Chronological Boundaries (1st ed.). John Wiley & Sons, Inc.

Schobben, M., Joachimski, M.M., Korn, D., Leda, L., & Korte, C. (2014). Palaeotethys seawater temperature rise and an intensified hydrological cycle following the end-Permian mass extinction. Gondwana Research, **26**(2), 675–683. doi: 10.1016/j.gr.2013.07.019

Schobben, M., Stebbins, A., Ghaderi, A., Strauss, H., Korn, D., & Korte, C. (2015). Flourishing ocean drives the end-Permian marine mass extinction. Proceedings of the National Academy of Sciences of the United States of America, **112**(33), 10298–10303. doi: 10.1073/pnas.1503755112 PMID: 26240323

Schobben, M., Ullmann, C.V., Leda, L., Korn, D., Struck, U., Reimold, W.U., Ghaderi, A., Algeo, T.J., & Korte, C. (2016). Discerning primary versus diagenetic signals in carbonate carbon and oxygen isotope records: An example from the Permian–Triassic boundary of Iran. Chemical Geology, **422**, 94–107. doi: 10.1016/j.chemgeo.2015.12.013

Sheng, H. (1988). New material of Early Permian ammonoids from Xizang and Qinghai. Professional Papers of Stratigraphy and Palaeontology, **2**, 76–84.

Shevyrev, A.A. (1965). Nadortyad Ammonoidea. In V.E. Ruzhencev & T.G. Sarytcheva (eds.), Rasvitie i smena morskikh organizmov na rubezhe Paleozoya i Mezozoya. Trudy Paleontologicheskogo Instituta Akademiya Nauk SSSR, 108, 166–182.

Shevyrev, A.A. (1968). Triasovye ammonoidei Yuga SSSR. Trudy Paleontologicheskogo Instituta Akademiya Nauk SSSR, **119**, 1–272.

Spath, L.F. (1930). The Eotriassic invertebrate fauna of East Greenland. Meddelelser om Grønland, **83**(1), 1–90.

Spinosa, C., Furnish, W.M., & Glenister, B.F. (1975). The Xenodiscidae, Permian ceratitoid ammonoids. Journal of Paleontology, **49**, 239–283.

Stampfli, G.M., & Borel, G.D. (2002). A plate tectonic model for the Paleozoic and Mesozoic constrained by dynamic plate boundaries and restored synthetic oceanic isochrons. Earth and Planetary Science Letters, **196**(1–2), 17–33. doi: 10.1016/S0012-821X(01)00588-X

Stepanov, D.L., Golshani, F., & Stöcklin, J. (1969). Upper Permian and Permian–Triassic Boundary in North Iran. Geolological Survey of Iran. Report, **12**, 1–72.

Teichert, C., Kummel, B., & Sweet, W.C. (1973). Permian-Triassic strata, Kuh-e-Ali Bashi, Northwestern Iran. Bulletin of the Museum of Comparative Zoology, Harvard University, **145**, 359–472.

Waagen, W.H. (1872). On the occurrence of Ammonites, associated with *Ceratites*, and *Goniatites* in the Carboniferous deposits of the Salt Range. Memoirs of the Geological Survey of India, **9**, 351–358.

Waagen, W.H. (1879). Salt Range fossils, 1. *Productus* Limestone fossils. Palaeontologia Indica, **1**, 1–85.

Zakharov, Y.D., & Pavlov, A.M. (1986). Permskie tsefalopody Primor'ya i problema zonal'nogo raschleneniya Permi teticheskoy oblasti. In Y.D. Zakharov & Y.I. Onoprienko (eds.), Korreliatsiya Permo-Triasovykh otlozhenii vostoka SSSR: 5–32.

Zakharov, Y.D. & Rybalka, S. (1987). Etalony permi i triasa Teticheskoy oblasti. In Problemy biostratigrafii permi i triasa Vostoka SSSR, DVNTs AN SSSR, 1987, 6–48.

Zhao, J., Liang, X., & Zheng, Z. (1978). Late Permian cephalopods from South China. Palaeontologia Sinica, Series B, **12**, 1–194.

Zheng, Z., & Chen, G. (1979). Upper Paleozoic Fossils. In Fossil Atlas of Northwest China, Qinghai, 2, 10–18.

Manuscript received: February 17th, 2019.
Revised version accepted by the Stuttgart editor: April 23rd, 2019.

Addresses of the authors:

Dieter Korn, Museum für Naturkunde Berlin, Leibniz-Institut für Evolutions- und Biodiversitätsforschung Invalidenstraße 43, 10115 Berlin, Germany & Nanjing Institute of Geology and Palaeontology, Chinese Academy of Sciences, 39 East Beijing Road, Nanjing, China;

e-mail: dieter.korn@mfn.berlin

Abbas Ghaderi (corresponding author), Nahideh Ghanizadeh Tabrizi Department of Geology, Faculty of Science, Ferdowsi University of Mashhad, Mashhad, Iran;

e-mail: aghaderi@um.ac.ir (corresponding author)
nahidehghanizadeh@gmail.com